Thermomigration and Electromigration in Zirconium*†

D. R. CAMPBELL‡ AND H. B. HUNTINGTON
Department of Physics and Astronomy, Rensselaer Polytechnic Institute, Troy, New York 12181
(Received 29 July 1968)

Experiments on directed atom motions in β-Zr have been carried out with a view to bringing additional experimental evidence to bear on the current conflicting theories of the anomalous diffusion behavior in this and other bcc refractory metals. Thermomigration and electromigration effects have been studied primarily by the surface-marker technique in zirconium wires purchased from the Materials Research Corp. (MRC) (purity 99.9%) and in rods supplied by the Oak Ridge National Laboratory (ORNL) (purity 99.98%). The thermomigration effects were large, with the mass flow to the hot (central) region of the specimens. The effective activation energy for this flow was 26±3 and 29±3 kcal/mole for MRC and ORNL Zr, respectively. These values are quite close to the activation energy for the so-called "low-temperature diffusion mechanism" ($Q=27.7$ kcal/mole) obtained from tracer diffusion data. If one assumes that this is the operative mechanism, then Q^*/f turns out to be -34 ± 11 kcal/mole. The fact that the forced motion shows no evidence of a high-temperature mechanism lends support to the hypothesis that this motion is primarily by dislocation, or short-circuit paths. The electromigration, on the other hand, is a very small effect for this material, with motion apparently toward the cathode. The activation energy is in the neighborhood of 30 kcal/mole, and the effective charge Z^*/f is about +0.3.

I. INTRODUCTION

FROM the rather extensive history of self- and impurity diffusion studies in fcc metals, a general pattern of diffusion behavior has been observed and is expressed in the form of several "rules" which when obeyed indicate a "normal" diffusion behavior. While most metals are found to be normal, there are several exceptions, and in regard to diffusion, these are referred to as "anomalous". The characteristics of normal metals are given as follows: The diffusion constant D, whether self- or impurity diffusion is indicated, can be expressed in the form

$$D=D_0e^{-Q/RT}, \tag{1}$$

where D_0 has a value within an order of magnitude of unity (units of cm²/sec), and the activation energy Q can be predicted to within ±20% by the melting-point rule

$$Q=34T_m \text{ cal/mole}, \tag{2}$$

where T_m is the melting point of the metal in °K. A plot of log$D$ versus $1/T$ is expected to be linear, implying that D_0 and Q are temperature-independent.[1]

In recent years, the interest in refractory materials has placed much emphasis on the properties of the high-temperature bcc metals. The diffusion behavior of several of them—i.e., Cr,[2] α- and δ-Fe,[3] Nb,[4] Mo,[5] Ta,[6] and W [7]—has been found to be normal. However, the high-temperature phases of four polymorphic bcc transition metals, namely, β-Ti,[8,9] β-Zr,[10,11] β-Hf,[12] and γ-U,[13,14] violate every criterion of normal behavior and are therefore considered to be anomalous. Excepting Hf, their Arrhenius plots (log$D$ versus $1/T$) are curved and over large portions of their temperature ranges, the activation energies are only half the value predicted by the melting-point rule. Further, their D_0's are 3–6 orders of magnitude too small. We might also list as anomalous the very large spread in impurity diffusion rates in β-Ti and γ-U [15] and the surprising increase of diffusion rates with pressure observed by Beyelev and Adda[16] for self-diffusion in γ-U and by Peart[17] for the diffusion of Fe in β-Ti.

The explanations which have been proposed follow

* Supported by contract with the U. S. Atomic Energy Commission.

† This paper is based on a thesis submitted to the Department of Physics and Astronomy at Rensselaer Polytechnic Institute, in partial fulfillment of the requirements for the Ph.D. degree, awarded to D. R. Campbell.

‡ Present address: I.B.M. T. J. Watson Research Center, Yorktown Heights, N. Y.

[1] See, for example, articles by A. D. LeClaire, D. Lazarus, and G. V. Kidson, in *Diffusion in Body-Centered Cubic Metals* (American Society for Metals, Cleveland, Ohio, 1965).

[2] J. Askill, in *Diffusion in Body-Centered Cubic Metals* (American Society for Metals, Cleveland, Ohio, 1965), p. 235.

[3] D. Graham and D. H. Thomlin, Phil. Mag. **8**, 1581 (1963).

[4] T. S. Lundy, J. I. Federer, R. E. Pawel, and F. R. Winslow, in *Diffusion in Body-Centered Cubic Metals* (American Society for Metals, Cleveland, Ohio, 1965), pp. 43–46.

[5] J. Askill and D. H. Thomlin, Phil. Mag. **8**, 997 (1963).

[6] R. L. Eager and D. B. Langmuir, Phys. Rev. **89**, 911 (1953).

[7] W. Dornberg, Metall. **15**, 977 (1961).

[8] J. J. Murdock, T. S. Lundy, and E. E. Stansbury, Acta Met. **12**, 1033 (1964).

[9] G. B. Gibbs, D. Graham, and D. H. Thomlin, Phil. Mag. **8**, 1269 (1963).

[10] G. V. Kidson and J. McGurn, Can. J. Phys. **39**, 1147 (1961).

[11] J. I. Federer and T. S. Lundy, Trans. AIME **227**, 592 (1963).

[12] F. R. Winslow and T. S. Lundy, Trans. AIME **233**, 1790 (1965).

[13] S. J. Rothman, L. T. Lloyd, and A. L. Harkness, Trans. AIME **218**, 605 (1960).

[14] Y. Adda and A. Kirianeko, Compt. Rend. Acad. Sci. Paris **247**, 744 (1958).

[15] N. L. Peterson and S. J. Rothman, Phys. Rev. **136**, A842 (1964).

[16] M. Beyelev and Y. Adda, in *Physics of Solids at High Pressure*, edited by C. Tomizuka and R. Emrick (Academic Press Inc., New York, 1965), p. 349.

[17] R. Peart, Phys. Status Solidi **20**, 545 (1967).

two main approaches, one focusing on extrinsic factors, the other on intrinsic properties.

In the extrinsic approach, D is considered to be the sum of two independent constants D_1 and D_2, which presumably describe the high-temperature (intrinsic) and low-temperature (extrinsic) mechanisms, respectively. Kidson[18] first proposed that the anomalous behavior may be due to the presence of a large temperature-independent concentration of vacancies arising from a strong vacancy-impurity interaction. (These metals, all of which are excellent "getters," usually contain several hundred ppm of interstitial impurities.) LeClaire[1] and Kidson[1] have suggested that these effects may be associated with an unusually large concentration of dislocations (presumably introduced by a martensitic-type phase transformation) which could provide many short circuit paths.

Neither of these models has won an unqualified acceptance. Kidson's impurity model requires that the vacancy-interstitial binding energy be about 30 kcal/mole. Unfortunately, there is yet no precedent for assuming such a large value. The dislocation model assumes dislocation densities of the order of 10^9 lines/cm^2 or greater depending on the particular material. Such values are several orders of magnitude higher than the densities which are known to exist in well-annealed normal metals. An alternative explanation is that these effects are entirely "intrinsic," i.e., they represent the true bulk diffusion properties of these metals. Askill and Gibbs[19] have suggested that two distinct point-defect mechanisms (e.g., divacancies and vacancies) may be making significant contributions to the total diffusivity. They argue that low-activation energies may occur for single-vacancy diffusion when there is relatively weak lattice binding as indicated by the large compressibilities[20] observed for some of the anomalous metals. The theory of intrinsic vacancies and divacancies has been further developed by Peart and Askill.[21] The low values of D_{02} which have been observed experimentally are discussed in terms of small values for ν (vibration frequency) and f (correlation factor). Gibbs has also argued[22] that negative entropies (and therefore low values of D_{02}) can occur if the increased vibration frequencies about the saddle-point configuration more than compensate for the lowering of frequencies about the relaxed vacancy. Aaronson and Shewmon[23] have employed a single-mechanism concept in attempting to relate the anticipated temperature dependence of an elastic constant, namely, $\frac{1}{2}(C_{11}-C_{12})$ in the vicinity of the bcc-hcp phase transformation to the activation parameters for vacancy diffusion. According to Shewmon,[24] if such an association is valid, then many of the anomalous features such as the decrease of activation enthalpy with temperature, negative and temperature-dependent activation entropies, and the increase of diffusion rate with pressure follow as logical consequences.

It appears that all of the models proposed are essentially speculative, since each requires one or more *ad hoc* hypotheses. It occurred to us that some additional clues for understanding the diffusion behavior of the anomalous metals might be obtained from suitably chosen thermomigration and electromigration experiments. Directed mass flow, whether due to thermal gradients (thermomigration) or electric fields (electromigration), presents some additional features to those available in a study of pure random motion (diffusion) which could throw some light on the effective atomic mechanism. In addition, the general apparatus used in directed motion studies is simpler to use at high-vacuum and high-specimen temperature than the usual diffusion gear since only the specimen is heated.

We have selected β-Zr as the material for study because precise reproducible diffusion measurements were available,[10,11] the curvature in the Arrhenius plot was very pronounced, the β phase exists over a large temperature range (nearly 1000°C), and the vapor pressure is relatively low so that long runs could be made at high vacuum without excessive evaporation.

A qualitative marker motion study of thermomigration in β-Zr and β-Ti has been reported by Feller and Wever,[25] where they observed that Zr atoms migrated toward the hotter regions. A preliminary account of our experiments has been reported elsewhere.[26] During the preparation of this final manuscript we were made aware of an independent investigation of thermomigration and electromigration in β-Ti and β-Zr carried out by Dübler and Wever, which has recently been published.[27] We are grateful to Dübler and Wever for the opportunity to study their manuscript before publication.

II. THEORY

Thermo- and electromigration studies involve the application of external forces, i.e., temperature gradient and electric field, respectively, which drive the matrix atoms and produce an atom flux which can be determined by measurement of dimensional changes in the specimens in which these forces are applied. The relationship between the matrix atom drift velocity and the applied force is given by the Nernst-Einstein equation

$$v_A = D_A F/kT, \tag{3}$$

[18] G. V. Kidson, Can. J. Phys. **41**, 1563 (1963).
[19] J. Askill and G. B. Gibbs, Phys. Status Solidi **11**, 557 (1965).
[20] J. Askill, Phys. Status Solidi **11**, K49 (1965).
[21] R. F. Peart and J. Askill, Phys. Status Solidi **23**, 263 (1967).
[22] G. Gibbs, Mem. Sci. Rev. Metl. **XLII**, 841 (1965).
[23] H. I. Aaronson and P. G. Shewmon, Acta Met. **15**, 385 (1967).
[24] P. G. Shewmon, Metallurgy Division, Argonne National Laboratory (private communication).
[25] H. Feller and H. Wever, J. Phys. Chem. Solids **24**, 969 (1963).
[26] D. R. Campbell and H. B. Huntington, Bull. Am. Phys. Soc. **11**, 185 (1966).
[27] H. Dübler and H. Wever, Phys. Status Solidi **25**, 109 (1968).

where D_A is the (uncorrelated) diffusivity of the migrating atoms, F the mean applied force, and T the absolute temperature.

A. Thermomigration

The thermomigration force which we have used in our analysis is given as

$$F_T=-(Q^*/N_A)\nabla T/T, \tag{4}$$

where N_A is Avogadro's number and Q^* is called the heat of transport and is the heat flow per mole that must be supplied in steady state to maintain unit molar flow. When the mass flow is by a vacancy mechanism a counter flow of vacancies is implicit and their enthalpy of formation appears as a negative term in the evaluation of Q^*. There are numerous treatments of the physical significance of Q^* in the literature,[28–35] and generally the conclusion has been that, for the vacancy mechanism, Q^* in large part is given by

$$Q^*\simeq\beta H_m-H_F, \tag{5}$$

where H_m and H_F are the molar enthalpies of migration, and formation for vacancies and β is a dimensionless factor with a value somewhere near but less than 1. The complete evaluation of Q^* requires understanding of all the factors inducing thermomigration (e.g., phonon flux, charge carrier flux, Thomson heat, etc.). A unified treatment of the respective roles of these factors has been attempted by one of us (HBH) elsewhere.[36] Substituting Eq. (4) into Eq. (3) and rearranging, we obtain

$$DQ^*/f=-v_ART^2/\nabla T. \tag{6}$$

In Eq. (6), D is the tracer self-diffusion constant and is equivalent to fD_A. The quantities v_A, T, and ∇T are determined experimentally, so that the product DQ^*/f is known. If D is also known from isotope studies and f can be calculated, then Q^* can be determined. We show later [Eq. (14)] that v_A may be written as $-v_m/\alpha$, where v_m is the measured velocity of surface markers. Using Eqs. (1) and (14) and taking the natural log of each side, one obtains from Eq. (6)

$$\ln\frac{DQ^*}{f}=\ln\left(\frac{v_m}{\alpha}\frac{RT^2}{\nabla T}\right)=\ln\frac{D_0Q^*}{f}-\frac{Q}{RT}. \tag{7}$$

Provided that Q^* and f are essentially temperature-independent, a plot of $\ln(DQ^*/f)$ versus $1/T$ should be linear, with slope $-Q/R$.

B. Electromigration

Under the application of an applied electric field, we write

$$F_E=Z^*|e|E, \tag{8}$$

where $|e|$ is the magnitude of the electron charge, and E the applied electric field strength, which can also be written

$$E=J\rho(T). \tag{9}$$

J is the current density and $\rho(T)$ the specimen resistivity. In general, the force $|e|Z^*E$ is made up of two components, one from the direct action of the electrostatic field and the other from momentum exchange with the charge carriers.

Repeating the steps used in Sec. II A, we obtain

$$DZ^*/f=v_AkT/J\rho(T)|e|. \tag{10}$$

Again, the quantities on the right are experimentally measured to determine DZ^*/f; Z^* is separated in the same way that was mentioned for Q^*. Similarly, we obtain

$$\ln\frac{DZ^*}{f}=\ln\left(-\frac{v_m}{|e|\alpha}\frac{kT}{J\rho(T)}\right)=\ln\frac{D_0Z^*}{f}-\frac{Q}{R}\frac{1}{T}. \tag{11}$$

C. Determination of Atom Drift Velocity

By measurement of local volume changes, which occur wherever the divergence of the vacancy flux is nonzero, we are able to calculate the flow of matrix atoms (or the counterflow of vacancies) throughout the specimen, provided we can discount the creation of voids. For cylindrical specimens, this requires measurement of changes in diameter and of surface-marker displacements as a function of position and time. Equating the rate of local volume change to the net influx of matter, we obtain for v_A, the atom drift velocity relative to the local lattice

$$v_A(x)=-\int_{x_a}^{x}[\dot{e}_l(x)+2\dot{e}_t(x)]dx. \tag{12}$$

The term in the brackets represents the volume dilatation rate. We shall refer to $\dot{e}_l$ as the longitudinal "strain" rate, where $\dot{e}_l=dv_m/dx$, and v_m is the surface-marker velocity. Likewise, $\dot{e}_t$ is called the radial "strain" rate $\dot{e}_t=R^{-1}dR/dt$, where R is the specimen radius; x_a refers to the position of the reference marker, where all strains are zero, i.e., there is no atom flux at x_a. The physical interpretation of Eq. (12) is that the mass flow through a cross section of the specimen will show as a dimensional change eleswhere in the specimen. If, as often happens, void formation does accompany forced atom flow, it may be possible to choose the

[28] D. O. Raleigh and A. W. Sommer, J. Chem. Phys. **36**, 381 (1962).
[29] P. G. Shewmon, *Diffusion in Solids* (McGraw-Hill Book Co., New York, 1963).
[30] W. Wirtz, Physik **XLIV**, 221 (1943).
[31] W. Shockley, Phys. Rev. **93**, 345 (1954).
[32] A. D. LeClaire, Phys. Rev. **93**, 344 (1954).
[33] J. A. Brinkman, Phys. Rev. **93**, 345 (1954).
[34] P. G. Shewmon, J. Chem. Phys. **29**, 1032 (1958).
[35] R. A. Oriani, J. Chem. Phys. **34**, 1773 (1961).
[36] H. B. Huntington, J. Phys. Chem. Solids **29**, 1641 (1968).

reference point x_a so that the integration with respect to x is over a void-free region, e.g., the anode side of a specimen undergoing electromigration by electrons.

Equation(12) can be slightly rewritten, since

$$\int_{x_a}^{x} \dot{e}_l(x)dt = v_m,$$

so that

$$v_A(x) = -\left[v_m + 2\int_{x_a}^{x} \dot{e}_l(x)dx\right]. \tag{13}$$

Elsewhere we have called $\dot{e}_l/(\dot{e}_l+2\dot{e}_t)$ the isotropy factor α. It is the ratio of the longitudinal strain rate to the dilatation rate and has a value of $\frac{1}{3}$ for an isotropic situation. While it is expected that $\alpha \geq \frac{1}{3}$, it has an upper value of 1 for the case where all dimensional changes are uniaxial. An elastic-plastic theory of α for cylindrically shaped specimens has been presented by Penney.[37] If α is a constant, independent of position, then

$$v_A(x) = -v_m(x)/\alpha. \tag{14}$$

Although the condition of constant α may not always be exactly valid for Zr, we shall use Eq. (14) as a reasonable approximation in the analysis of our results.

III. EXPERIMENTAL PROCEDURE

A. Material

Zirconium samples were obtained from two sources. Wires of 0.050-in. diameter were purchased from Materials Research Corp., Orangeburg, N. Y., and rods of 0.137-in. diameter were loaned to us from the Oak Ridge National Laboratory.[38] The MRC zirconium was prepared by cold swaging singly zone-refined Zr rods, and was supplied with the following analysis:

carbon	20 ppm	silicon	5 ppm
iron	10 ppm	magnesium	5 ppm
nickel	10 ppm	hydrogen	10 ppm
chromium	10 ppm	nitrogen	10 ppm
aluminum	10 ppm	oxygen	200 ppm

The ORNL rods were prepared by cold swaging triply zone-refined stock. They were not analyzed but were expected to contain less than 30 ppm oxygen, less than 30 ppm total metal impurities, and approximately 100 ppm Hf.

B. Apparatus

In our experiments, high-purity Zr rods were resistively heated with direct current in the vacuum system shown in Fig. 1. The samples were mounted between two water-cooled copper clamps, one fixed and the other free to translate along the specimen axis so the specimen could undergo dimensional changes in a stress-free manner. The free electrode was immersed in liquid gallium alloy for electrical and thermal contact.

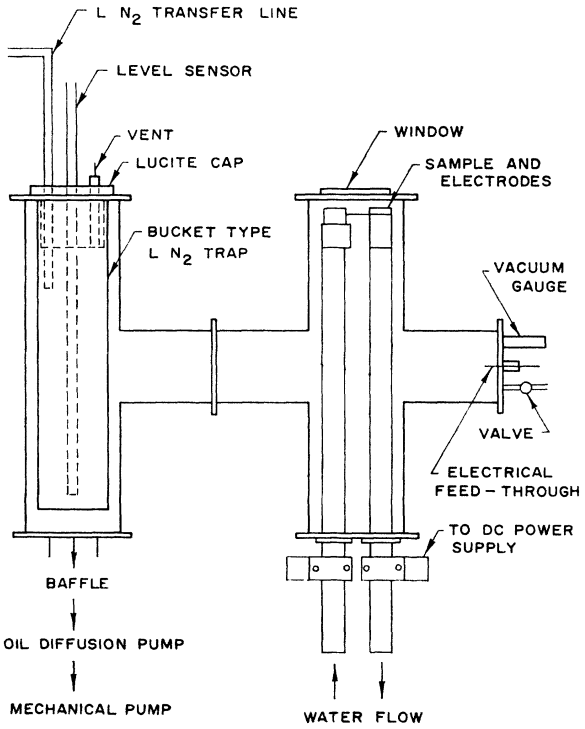

FIG. 1. Experimental apparatus.

The vacuum chamber was constructed of stainless steel and glass and was gasketed with bakeable elastomer O rings. A large liquid-nitrogen trap was built into the chamber to prevent diffusion-pump oil contamination and also to help pump down the system. The spstems operating pressure was 2×10^{-8} Torr or less after a 14-h bakeout at about 120°C.

Specimen dimensional changes, both longitudinal and radial, were measured with a Gaertner traveling microscope, which was mounted above the sample, the latter being observed continually during a run through a glass window. The microscope screw axis was aligned along the specimen axis so that surface-marker positions could be recorded with an accuracy of about ± 3 μ. Radial dimensions were observed using a filar micrometer eyepiece in the microscope and could be made to about the same accuracy.

The specimen temperature distribution was obtained by use of a calibrated light-sensitive CdS resistor, which could be mounted in the traveling microscope to measure temperature versus position. This technique of temperature measurement was originally developed by Hehenkamp,[39] and has a temperature resolution easily less than 5°C throughout the entire temperature range.

[37] R. Penney, J. Phys. Chem. Solids **25**, 335 (1964).

[38] We are indebted to J. C. Wilson, Metals and Ceramics Division, for the preparation and loan of this material.

[39] Th. Hehenkamp, Rev. Sci. Instr. **33**, 229 (1962).

The Zr specimens were heated by means of a 300-A dc power supply, which was regulated to maintain a constant voltage across the specimens. For well-annealed samples this method was capable of temperature control to ± 10°C over a 24-h period, but required periodic adjustments over longer intervals to maintain these limits.

C. Procedure

1. Sample Preparation

Zirconium samples were cut to the desired length (1–2 cm for the MRC wire, $1\frac{1}{2}$ in. for the ORNL rods), then etched vigorously in a solution of 5% HF, 30% HNO_3, and 65% H_2O (by volume) to remove surface contamination. Surface markers were made by drawing, in one steady stroke, a steel razor blade transversely across the specimen to produce a marker about 50–100 μ wide and the same distance deep. The samples were carefully mounted in the vacuum chamber, which was then sealed, pumped down, and baked out. After cooling and reaching the correct operating pressure, the samples were heated to run temperatures in a period of 1–3 h, depending on the individual run. For low-temperature runs ($T \leq 1500$°C) specimens were annealed for 1 day at the run temperature. For higher-run temperatures, they were annealed slightly below 1500°C for 1 day, then slowly brought to run temperature, where they were annealed several additional hours before initial readings were taken.

2. Temperature Calibration: Control and Measurement

The photoresistor was calibrated according to the technique devised by Hehenkamp,[39] using welded thermocouples of W, 3% Re(+) and W, 25% Re(−) wires supplied by Engelhard Co., Newark, N.J. Once the sample was at the desired run temperature as determined from the photoresistor reading at the specimen center, we could maintain a constant voltage across the specimen by means of a feedback controller which sensed the dc voltage across the specimen and adjusted the power-supply output accordingly. This method produced temperature control to within ± 10°C as long as the specimen resistance was not changing rapidly, as was certainly true after annealing. However, to adjust for long-term resistance changes, the temperature was checked each day and the power-supply settings adjusted when necessary. Below a maximum temperature of 1500°C, this procedure was quite adequate to maintain the stated temperature limits, but for the higher-temperature runs a serious difficulty was encountered because of evaporation of the zirconium. The evaporated metal atoms condensed on the chamber viewport, thereby reducing the light intensity reaching the photoresistor, which in effect made the temperature measurement read too low. An evaporation shield was installed to keep the viewport clean but it did not completely solve this problem because the windows was still coated with Zr while dimensional changes or the temperature distribution were being measured. We overcame this difficulty by calibrating the maximum temperature of a well-annealed sample versus power input to it before the viewport became coated to any appreciable extent. For runs below 1500°C maximum temperature, the temperature distribution was measured near the beginning and end of the run and the average values of temperature used at each position. For the high-temperature runs, the initial temperature distribution was used. The values of T versus position were computer-fitted with a least-squares parabola, and the fitted curve used to compute T and ∇T.

3. Measurement of Dimensional Changes

To determine the longitudinal strain rates, marker positions were measure periodically during each run. Radial measurements were made by two methods: (a) at the beginning and end of the run, with the sample in place and "at temperature," or (b) before and after the run with the sample outside the chamber and at room temperature. Method (a) avoids deformations which may be caused by heating and cooling through the phase transformation but cannot detect deviations from a circular cross section; these can be detected by method (b) if two sets of diameters, at 90° to each other, are measured.

IV. RESULTS

A. Thermomigration

We determined the velocity of each marker by eye or by least-squares fits of marker displacements versus time. Figure 2 shows typical results.

Marker velocity versus position and rate of radial change for a low-temperature run (run 13-*l*, where T_{max} was ~954°C) is shown in Fig. 3, while a similar graph for a high-temperature run (run 2-*l*, where T_{max} was ~1503°C) is shown in Fig. 4.

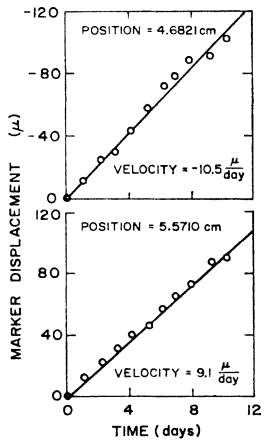

FIG. 2. Marker displacement versus time for run 1-*l*.

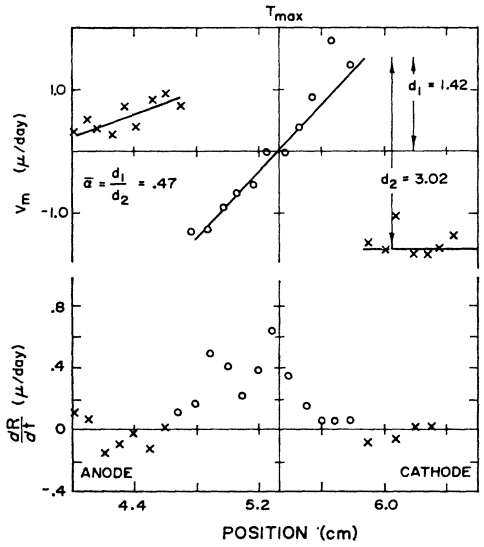

FIG. 3. Marker velocities and rates of radial dimension changes versus position for run 13-l (×—α phase, ○—β phase).

Figure 5 presents marker velocity versus position for two runs that were identical except for the prerun annealing procedure, in order to demonstrate the affect of annealing on atom drift velocity.

Values of $\ln(DQ^*/f)$ have been computed from Eq. (7) and plotted versus $1/T$ in Figs. 6 and 7 for ORNL and MRC zirconium, respectively. Marker velocities used in Eq. (7) were obtained from the antisymmetric portions of v_m versus x plots. Values of T and ∇T were taken from least-squares fits of T versus x, where T was measured with the photoresistor at the position of each marker. (All computations were carried out on an

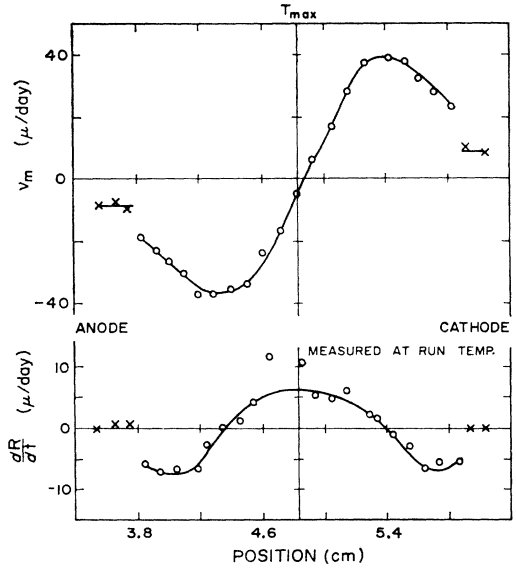

FIG. 4. Marker velocities and rates of radial dimension changes versus position for run 2-l (×—α phase, ○—β phase).

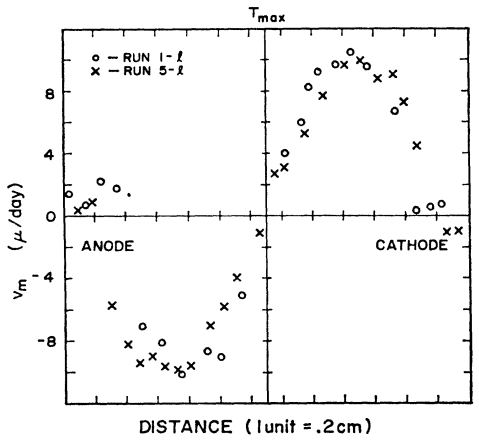

FIG. 5. Simultaneous plot of marker velocities versus position for runs 1-l and 5-l.

IBM 1620 computer.) We have used α values of 0.65 and 0.47 for the ORNL and MRC material, respectively. (See discussion, Sec. V.) The data presented in these graphs were screened as follows: Only points in the defect "source" regions were used, since α in the defect "sink" regions was somewhat uncertain. (See Sec. V.) We also excluded points very close to the temperature maximum because the combined error due to the ratio $v_m/(\partial T/\partial x)$ is very large there. Finally, points deviating from the smooth curve by more than ± 3 average deviation were excluded.

The data have been computer-fitted with least-squares lines which are given by

$$\text{ORNL Zr: } DQ^*/f = -2.2\times 10^{-4} e^{-(29\,000\pm 3000\ \text{cal/mole})}\ \text{cm}^2/\text{sec}, \quad (15)$$

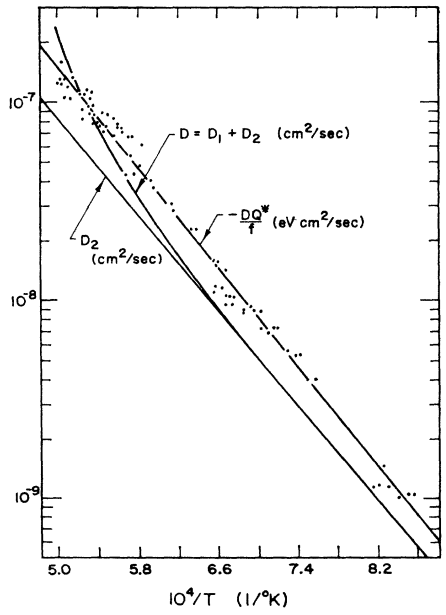

FIG. 6. Log$(-DQ^*/f)$ and log$D$ versus $1/T$ for ORNL Zr.

MRC Zr: DQ^*/f

$$=-7.8\times10^{-5}e^{-(26\,000\pm3000\ \text{cal/mole})/RT}\ \text{cm}^2/\text{sec}. \quad (16)$$

Activation energies for these plots are found to be 29±3 kcal/mole over the temperature range 900 to 1740°C for ORNL specimens and 26±3 kcal/mole for MRC specimens. The D $(=D_1+D_2)$ values from tracer self-diffusion studies are also shown for the sake of comparison.[11]

The calculation of Q^*/f was made by assuming that either D_2 or D_1+D_2 represents "D" in Eqs. (15) and (16), where D_1 and D_2, the intrinsic and extrinsic diffusion constants respectively, were calculated by Kidson[18] from the combined data of Kidson and McGurn[10] and Lundy and Federer.[40]

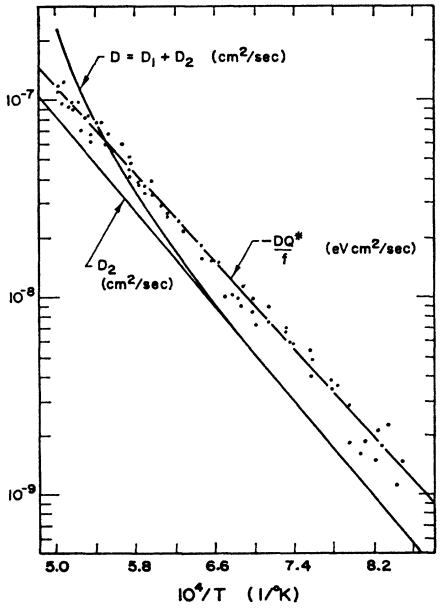

FIG. 7. Log$(-DQ^*/f)$ and log$D$ versus $1/T$ for MRC Zr.

$$D_1=1.34e^{-(65\,200\ \text{cal/mole})/RT}\ \text{cm}^2/\text{sec}, \quad (17)$$

$$D_2=8.5\times10^{-5}e^{-(27\,700\ \text{cal/mole})/RT}\ \text{cm}^2/\text{sec}. \quad (18)$$

In Fig. 8 we have plotted Q^*/f versus T for the ORNL zirconium for the two assumed values of D mentioned above. The mean value of Q^*/f for $D=D_2$ is -34 ± 11 kcal/mole.

B. Electromigration

The electromigration effect in Zr was found to be quite small and therefore difficult to separate from the much greater thermomigration. In Figs. 9, 10(a), and 10(b) we present data demonstrating two techniques which we used to determine the electromigration. Figure 9 shows v_m versus x for run 12-l. During this run

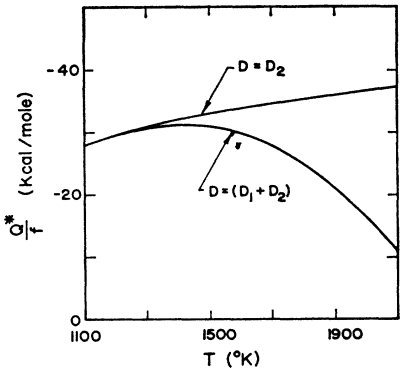

FIG. 8. Q^*/f versus T for $D=D_2$, D_1+D_2.

the direction of current was reversed after the marker velocities were well established, and the run was continued with the new direction of current. The two curves obtained are shown and the sense of electromigration clearly indicated. In Fig. 10(a) we have plotted v_m versus x for run 3-l. This curve has been separated into symmetric and antisymmetric parts, Fig. 10(b), and these can be attributed to the electromigration and thermomigration, respectively. The $v_m=0$ line in Fig. 10(a) is placed half-way between the values of the reference end markers in the two α-phase regions. Of course the positioning of this line is very crucial in determining the electromigration contribution.

We have computed values of $\ln(DZ^*/f)$ from Eq. (11), using marker velocity obtained from the symmetric parts of smoothed marker velocity plots of runs 3-l [Fig. 10(b)] and 9-l (data not shown). For $\rho(T)$ we have used a mean value of 130 $\mu\Omega$ cm,[41] since the temperature variation of ρ over the temperature range of interest is only 3%. These runs were made on ONRL zirconium so the value of 0.65 was used for α. In Fig. 11 we show DZ^*/f versus $1/T$ for these data, along with the tracer self-diffusion data for compaarison. The electromigration data can be expressed by the relation

$$DZ^*/f=6\times10^{-5}e^{-(31\,000\pm5000\ \text{cal/mole})/RT}\ \text{cm}^2/\text{sec}. \quad (19)$$

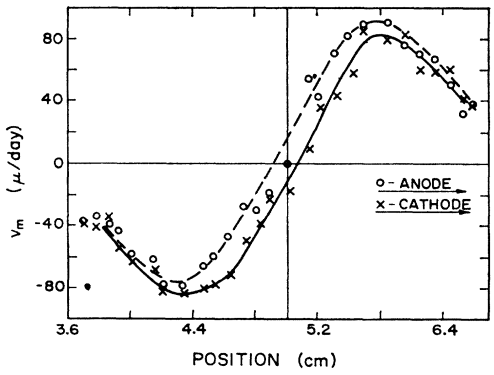

FIG. 9. Effects of current reversal for run 12-l.

[40] T. S. Lundy and J. I Federer, Oak Ridge National Laboratory Report No. ORNL-3339, 1962 (unpublished).

[41] *Handbook of the Thermophysical Properties of Solid Materials* (The Macmillan Co., New York, 1960).

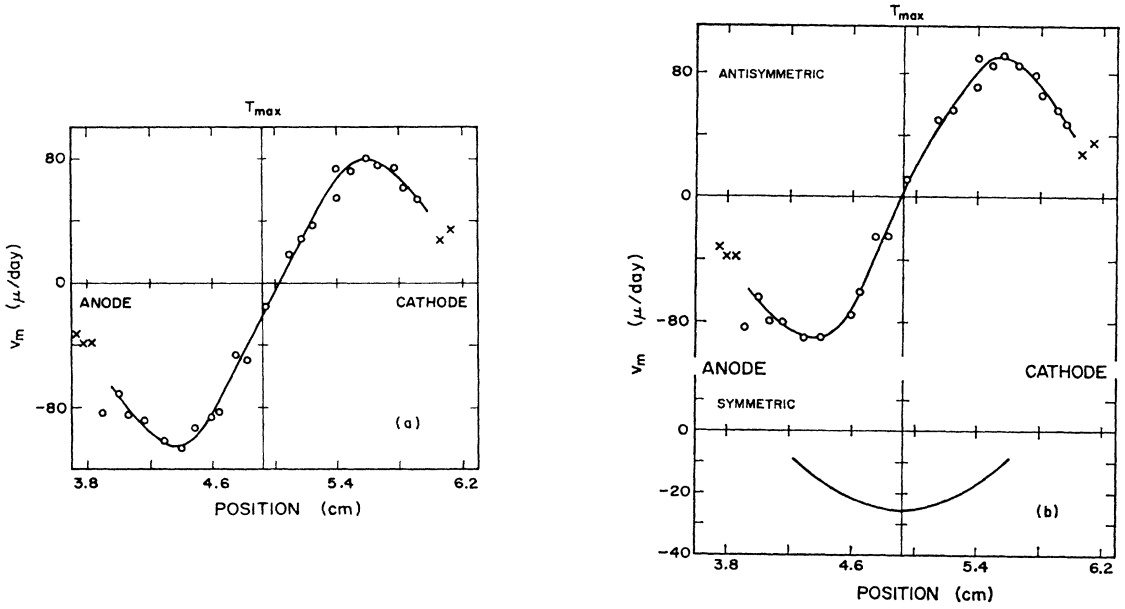

FIG. 10. (a) Marker velocities versus position for run 3-*l* (×—α phase, ○—β phase); (b) antisymmetric and symmetric contributions to v_m for run 3-*l* (×—α phase, ○—β phase).

In Fig. 12, we show Z^*/f computed by assuming either D_2 or D_1+D_2 represents D in Eq. (19). Assuming that only D_2 contributes to electromigration, we obtain $Z^*/f=+0.3\pm0.1$. The positive sign for Z^* is consistent with measurements on the Hall coefficients in the α phase.[42] For β-Zr there appear to be no reported results.

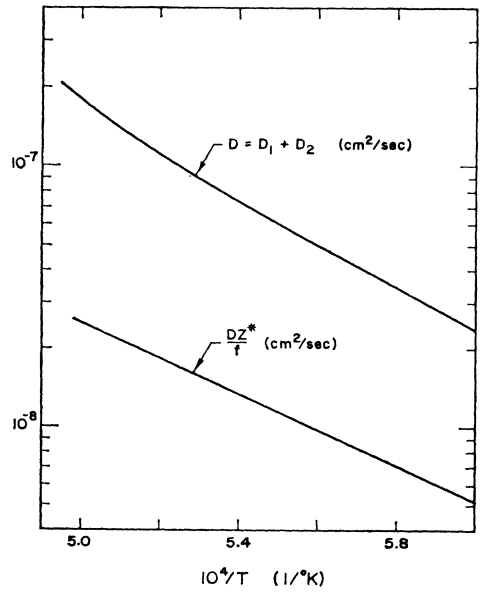

FIG. 11. Log(DZ^*/f) versus $1/T$.

[42] United Kingdom, Atomic Energy Commission TRG Report No. 108(R) (unpublished).

V. DISCUSSION

A. Interpretation of the Marker Velocity versus Position Graphs

The graphs have been constructed using the convention that velocities toward the right (fixed end) are positive while velocities to the left (free end) are negative. A positive slope indicates local expansion, i.e., mass accumulation both radially and longitudinally and a negative slope the opposite. A region of mass accumulation implies a vacancy source, since we assume that thermodynamic equilibrium of vacancies holds everywhere in the sample.

In Fig. 3 we note an over-all sample contraction (i.e., the free end has a positive velocity) while the opposite is true in Fig. 4. Contraction occurs at the α-β interface because defects which were created in the hot center

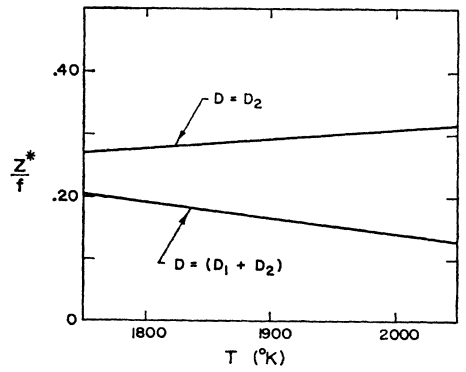

FIG. 12. Z^*/f versus T for $D=D_2$, D_1+D_2.

region in a more or less isotropic fashion, i.e., $\frac{1}{3} \leq \alpha$, were annihilated at the phase boundary nearly uniaxially, i.e., $\alpha \simeq 1$. This is due to the much reduced defect mobility in the α phase. Expansion occurred because defect "sink" regions (negative slope of v_m versus x) were characterized by α's smaller than those in the defect "source" regions (positive slope). (See Sec. V B.) A detailed treatment of these expansion and contraction effects and some observations on void formation in β Zr will be published elsewhere.

We correct for the expansion or contraction of the samples by drawing a horizontal base line midway between the reference points at either end of the sample. Marker velocities measured from this line refer to a coordinate system fixed to the sample and are therefore velocities relative to the sample's center of mass.

B. Determination of α Factor

From radial measurements, we have observed that the α factor remains approximately constant in the defect source region (the central portion of the sample) but appears to vary in the sink regions near the phase boundary. This effect may be due to a stress field near the phase boundary which perturbs the flow of defects[43] or possibly due to defect supersaturation in the sink region.

Experimental difficulties prevented extensive radial measurements, which are needed to determine α. Reasonably accurate α determinations for the source region were made on ORNL samples in runs 1-*l* and 2-*l*, where $\alpha \simeq 0.65$ in both cases. Determinations of α from scattered data in several other runs on ORNL Zr also were compatible with this value. We have used $\alpha \simeq 0.65$ in all our calculations for ORNL Zr. For the MRC samples, α was not measured, but we have deduced a value of 0.47 by "forcing" agreement between the least-squares lines of $\ln(DQ^*/f)$ versus $1/T$ for the two types of samples.

An alternative determination of α can be made if the temperature distribution is imposed in such a way that the defect sink regions are entirely eliminated from the specimen. Referring to run 13-*l* in Fig. 3, the source region α can be obtained from the ratio of the rate of expansion of $\frac{1}{2}$ the β-phase segment d_1 to the rate of contraction at the boundary d_2. The α value here was determined as 0.47 by this method. A similar calculation was made for MRC Zr in run 4-*S* (not shown) and basic agreement with the MRC value chosen was obtained.

The smaller value for α for the MRC Zr specimen is probably a consequence of small-specimen diameter rather than any intrinsic difference between the MRC and ORNL materials. The shape dependence of α is clearly evident in Penney's analysis.[37]

[43] J. D'Amico, Rensselaer Polytechnic Institute (private communication).

C. Influence of Gaseous Impurities

To minimize the effects due to pickup of gaseous impurities, all runs were made in a moderately high vacuum. Furthermore, we employed direct current in order to "electromigrate out" gaseous impurities from the center of the specimen. The purification effect by dc has been verified by previous experiments at high temperatures.[44] In bcc Zr, oxygen migrates rapidly toward the anode, presumably from octahedral to octahedral site.[45]

The influence of impurities, as revealed by asymmetry in the marker velocity plots, was undetected in all but one run. In run 13-*l*, which was run for 19.4 days, a weight increase of 0.018% was observed. (This was a run at low temperature where no evaporation occurred.) If we assume this contamination is due to oxygen, then this pickup amounts to 46 ppm accumulation per day. Since O atoms migrate toward the anode, we expect them to accumulate at the phase boundary and also to be absorbed into the α phase on the anode side. In Fig. 3, it is apparent that the anode side α phase has expanded (positive slope) at a uniform rate during the run, and that the velocity graph is not perfectly antisymmetric about the temperature maximum (geometric center). The contraction rate occurring at the phase boundary on the anode side is significantly less than the contraction rate on the cathode side, and this may be due to the buildup of a relatively high concentration of oxygen at the phase boundary together with void formation. Metallographic examination revealed slight porosity in the β phase adjacent on the anode side. No evidence for porosity was found near the cathode side.

The asymmetry referred to above amounts to only a few tenths of a micron per day, and is unnoticeable in higher-temperature runs due to both their shorter duration (i.e., less impurity accumulation) and to their proportionately greater marker velocities, i.e., all other runs had velocities 1–2 orders greater than run 13-*l*.

At higher temperatures, evaporation of the metal prevents correlation of weight changes with impurity accumulation.

D. Influence of Preanneals

We studied the influence of dislocations on the diffusion parameters by performing identical runs while altering the prerun heat treatment of the specimens in order to vary the dislocation densities in each run. In addition, the time dependence of the marker velocities was continuously observed to detect any transient behavior which might occur due to annealing of defects.

In order to test the effect of extended high-temperature anneals, we annealed the Zr specimen (run 5-*l*) for

[44] J. deBoer and J. Fast, Rec. Trav. Chem. **55**, 459 (1939); **59**, 161 (1940).

[45] B. Lustman and R. Kerze, *Metallurgy of Zirconium* (McGraw-Hill Book Co., New York, 1955).

72 h at $T_{max}=1740°C$, then slowly cooled to room temperature and put the markers (razor scratches) on the sample. We then heated it to a T_{max} of 1500°C for 12 h, followed, after slowly cooling to 1250°C, by a 6-day run at this temperature. The first anneal was done to eliminate cold-work defects in the ORNL material as supplied and to provide a large grained mechanically stable β phase. (Markers were made on the sample after this very-high-temperature anneal to prevent their being washed out by surface diffusion and evaporation.) The second anneal at 1500°C was performed to stabilize or remove defects introduced by passing twice through the phase transformation, and was done at the highest temperature possible without incurring serious distortion in marker shape.

The results of runs 5-*l* and 1-*l* are compared in Fig. 5. Run 1-*l* was performed by heating a cold-worked specimen (as supplied by ORNL) directly to a maximum temperature of 1250°C, where it was maintained for 10 days. It is clear from Fig. 5 that there is no significant difference in the marker velocities determined from these two runs. In Fig. 2, we show marker velocity plots from run 1-*l*. Their linearity is taken as evidence that stable defect concentrations prevailed during the course of the run.

E. Analysis of Experimental Errors

The relative errors in v_m, T, and $\partial T/\partial x$ are estimated to be ± 10, $\pm\frac{1}{2}$, and $\pm\frac{1}{2}\%$, respectively, and are assumed random. For a large number of data points such as in Figs. 6 and 7, these errors have a relatively small effect on the least-squares values for Q and DQ^*/f. However, data from some of our runs [12-*l* (not shown) and 13-*l*] lead us to suspect that the α factor may vary as much as $\pm 20\%$ from the value of 0.65 determined from 1-*l* and 2-*l*. This situation can introduce a systematic error in the set of data points for a particular run. This idea correlates with our observation that the calculated activation energy varies by roughly $\pm 10\%$ [if one deletes the data for a suspect run (e.g., 12-*l*) in the least-squares analysis]. Therefore the 10% figure is used to estimate errors in Eqs. (15) and (16).

Our estimate of the errors in Q^* is also qualitative. Again the uncertainty in α for those samples when it was inferred rather than measured injects a relative error of $\pm 20\%$ for DQ^*/f. It remains now to assess the influence of the uncertainty in D on the quantity Q^*/f. If one examines the independent diffusion data of Kidson and McGurn[10] and Federer and Lundy,[11] one concludes that diffusion measurements in β-Zr are reproducible to roughly $\pm 10\%$. Assuming this to be error for Kidson's[18] estimate of D, we arrive at a total error for Q^*/f of $\pm 30\%$.

For the electromigration experiments, the error in Q, Eq. (19), has been estimated from the possible variation in carrying out the antisymmetrization of the v_m versus x graphs. The error estimate of $\simeq\pm 40\%$ in Z^*/f was calculated, assuming errors of $\pm 10\%$ in D, $\pm 20\%$ in α, and $\pm 10\%$ in v_m.

F. Significance of Investigation

In the Introduction it was pointed out that a variety of mechanisms have been examined by several authors as a possible explanation for D_2. A representative listing of mechanisms could include the extrinsic vacancies of Kidson,[18] the intrinsic vacancies of Askill and Gibbs[19] and those of Aaronson and Shewmon,[23] other point defects such as divacancies, interstitials and interstitialcies and structural defects, e.g., dislocations or grain boundaries. Of course, ring mechanisms are ruled out, at least for D_2, by the occurrence of marker movements indicating net mass transfer in the diffusion process.

Although the anomaly of diffusion in Zr is still far from understood, the present investigation has, we feel, somewhat narrowed the field of possibilities. The fact that the activation energy for both forced motions, thermomigration and electromigration, agreed within experimental error over the whole temperature range of the β phase with the slope of the low-temperature part of the curved Arrhenius plot for the diffusion measurement seems to rule out the possibility that the curvature can be explained by a single mechanism with temperature-dependent Q. Of the extrinsic mechanisms the impurity-associated vacancy seems quite unlikely in view of the negative results obtained by Askill[46] looking for impurity effects and our own results, which showed that the extent of the atom motion and its sustained uniformity in time could not be attributed to any impurity especially susceptible to thermomigration.

Another intrinsic mechanism, that of the low-temperature vacancy–high-temperature divacancy has been suggested by Askill and Gibbs[19] and strongly urged by Askill and Peart.[21] The principal difficulty here is to explain why D_0 should be so much larger for the divacancy. Also to be explained is why the divacancy makes negligible contribution to the thermomigration. On the grounds of the usual Wirtz model [see Eq. (5)] one would expect the divacancy, with its larger formation energy and smaller energy of motion, to have a more negative Q^* than the single vacancy. A possible answer here may lie in the contribution of the charge carriers to the thermomigration force. It is now believed that under certain circumstances, such as for the transition elements platinum and cobalt, the large thermomigration has its origin in the charge-carrier moving-atom collisions. One could imagine that the activated complex for the divacancy might scatter the electrons less strongly than would the corresponding configuration for the single vacancy.

The possibility that such structural defects as grain boundaries play an important role in D_2 seems unlikely. In β-Zr, the presence of very large grains in Federer and

[46] J. Askill, Phys. Status Solidi **16**, K63 (1963).

Lundy's[11] samples and in our own indicate that grain-boundary diffusion cannot be playing a significant role. In our case, the roughly 2-cm β-phase segment of each sample was usually found to consist of three or four grains whose boundaries were effectively normal to the direction of mass flow. On the other hand, Lundy, Federer, Pawel, and Winslow[4] have recently demonstrated the enhanced diffusion of Nb in Ta due to substructure (dislocation arrays).

If we assume that dislocations are responsible, then according to the theory of Hart[47]

$$D=(a\rho/d)D_{\text{disl}}, \tag{20}$$

where ρ is the dislocation density, a is an effective "cross section" in terms of the number of sites characterized by D_{disl}, and d is the site density of the perfect crystal. D_{disl} is often assumed to have a preexponential factor of unity (units of cm^2/sec) and an activation energy of approximately $\frac{1}{2}$ that required for bulk diffusion. The assumptions are prompted by the classic Turnbull and Hoffman study of self-diffusion of Ag along grain boundaries and dislocations arrays.[48,49] The site density of the perfect crystal is $\sim 10^{15}$ sites/cm^2, and D_{02} has been calculated by Kidson[18] to be $\sim 10^{-5}$ cm^2/sec. For the a values of 1, 10, and 100 sites/line, Eq. (20) gives corresponding ρ values of $\sim 10^{10}$, $\sim 10^{9}$, and $\sim 10^{8}$ lines/cm^2. The postulation of such a dense dislocation network, stable as we have seen to nearly 1750°C, is certainly a weakness in this explanation.

The dislocation model, on the other hand, is strongly suggested by other results in our investigations since it provides a ready answer why the parameters of the directed motions show only one activation energy. (This is clearly true of Q^*/f and apparently true of Z^*/f within the limited accuracy of the latter measurements.) The answer hinges on the small value for f to be expected for a dislocation mechanism so that uncorrelated directed motion tends to be dominated by the dislocation transport over a wider range of temperature than is the case for the straight diffusion. This idea was first emphasized by Wever[50] and applied by him and Hering to their investigation of mass transport in γ-iron.[51] Again, the study of electromigration of Ni in Cu by Stepper and Wever[52] bears out this concept. In an intuitive way one can imagine how vacancies might move very readily along a dislocation contributing substantially to mass transport without bringing about any atomic mixing by diffusion. Alternatively, one can take the point of view that the value of f can be estimated roughly from the relation $f=1-2/z$, where z is the number of next neighbors to the vacancy that can interchange with it. If one takes z to be 2 for a vacancy on a dislocation, it is apparent how the corresponding f value could be really small!

In the case of Zr there is direct experimental evidence from isotope measurements by Graham[53] on the diffusion of Zr in β-Zr, quoted by Peart and Askill,[21] that shows the quantity $f(\Delta K)$ is of the order of 0.1. The quantity (ΔK) is defined as the fraction of the kinetic energy which rides with the jumping atom in the unstable normal mode at the saddle point for a vacancy jump. It is a quantity which enters critically into the theory of the isotope effect in diffusion and is generally believed to be near unity, particularly in the close-packed lattices. There is experimental evidence for smaller (ΔK) in bcc lattices, e.g., Na.[54] ($\Delta K \sim 0.5$.) One concludes that independent experimental evidence confirms the small value of $f(\sim 0.2)$.

The smallness of f also helps to explain the large observed value of Q^*/f, namely, -34 ± 11 kcal/mole. If we go now to Eq. (5) and take H_m and H_f to refer to the low-temperature process then this sum should be Q_2 or 28 kcal/mole. If we take them to be approximately equal and put $f\sim 0.2$ then one obtains agreement for Q^* with $\beta\sim 0.5$. Of course these numbers are merely reasonable guesses; they only serve to show that Q^* is not outside the bounds of expectation.

If one turns now to Z^*/f, which was measured at 0.3 ± 0.1, the same choice for f gives a Z^* of 0.06 which is certainly the smallest yet observed. Apparently in this metal there is a very close compensation between the electrostatic force and the net drive contributed by the holes and electrons. Possibly the balance is delicate enough to be reversed by very dilute impurity or changes in substructure. In any case, a negative (electron-driven) Z^* has been reported in a similar investigation by Dübler and Wever.[27]

VI. CONCLUSIONS

Into the highly controversial topic of the mechanisms for atomic motions in the anomalous bcc metals we have attempted to introduce additional experimental material from the study of forced motion in one such metal, zirconium. The evidence from our work indicates only one mechanism is involved in the forced motions as contrasted with the situation for diffusion where two activation energies are clearly indicated. The argument against a temperature-dependent activation energy to explain the diffusion result appears strong.

The question naturally arises why does the low-temperature mechanism dominate the forced motions but not the random. We are inclined to believe that the answer lies in a mechanism for which the correlation coefficient will be very small. Since in our work we observe the uncorrelated D, it is quite possible for such

[47] E. Hart, Acta Met. 5, 597 (1957).
[48] D. Turnbull and R. Hoffman, Acta Met. 2, 419 (1954).
[49] R. Hoffman and D. Turnbull, J. Appl. Phys. 22, 634 (1951).
[50] H. Wever, Acta Met. 15, 443 (1967).
[51] H. Hering and H. Wever, Acta Met. 15, 377 (1967).
[52] J. Stepper and H. Wever, J. Phys. Chem. Solids 28, 1103 (1967).
[53] D. Graham, quoted from Ref. 21.
[54] L. W. Barr and J. N. Mundy, in *Diffusion in Body-Centered Cubic Metals* (American Society for Metals, Cleveland, Ohio, 1965), p. 171.

a mechanism to dominate at all temperatures. Both the dislocation model and the "vacancy" model of Peart and Askill can account for a small correlation factor. However, the authors are somewhat more disposed toward the dislocation model, particularly since it can explain the analogous thermomigration and electromigration observed in γ-Fe.[21] Low values for D_{02} and Q_2 also find an easy explanation in the dislocation model. The weakness of this hypothesis is the need to postulate an extensive dislocation network formed during the phase transformation and unexpectedly stable under annealing treatment. Until there is direct experimental observation to the contrary, we are inclined to hold to this explanation, although the single vacancy, divacancy model[21] is also still a possibility.

ACKNOWLEDGMENTS

The authors express their gratitude to John F. D'Amico for his assistance with the measurements. We also thank Dr. George Ansell for several enlightening discussions.

PHYSICAL REVIEW VOLUME 179, NUMBER 3 15 MARCH 1969

Pressure Calculations and the Virial Theorem for Modified Hartree-Fock Solids and Atoms*

MARVIN ROSS
Lawrence Radiation Laboratory, University of California, Livermore, California 94550
(Received 23 September 1968)

An expression for the pressure of a Hartree-Fock-Slater solid is derived. It is shown that for this expression only those forms of the local exchange potential that are rigorously derived from the variational principle will give meaningful results in pressure calculations.

I. INTRODUCTION

IN a large number of the calculations made for the electronic energy levels of atoms and solids, a modified form of the Hartree-Fock equations is used. The modification is generally that of replacing the nonlocal Hartree-Fock exchange terms, which are difficult to calculate, by a local exchange potential $V_{ex}(r)$, which is proportional to the $\frac{1}{3}$ power of the local electron density $\rho(r)$, or $V_{ex}(r)=C[\rho(r)]^{1/3}$. In the Kohn-Sham approximation,[1] C is $(3/\pi)^{1/3}$, and in the Slater approximation[2] it is larger by $\frac{3}{2}$.

The present paper treats the problem of calculating pressure for a system described by the modified Hartree-Fock equations and, in particular, considers just what bearing the derivation of the one-electron exchange term has on the rigorously correct formulation of the pressure.

It will be shown that the pressure of a solid may be determined by the modified Hartree-Fock method, using a form of the virial theorem in which $PV=\frac{2}{3}T+\frac{1}{3}U$. The terms P, V, T, and U are, respectively, pressure, volume, average kinetic, and potential energy for the solid. For the case of free atoms, $2T=-U$.

It will also be shown that this theorem can give meaningful results only when applied to those cases in which the one-electron eigenvalue equations have been derived from the expression for the total energy, using the variational principle rigorously. This is so in the case of the Kohn-Sham approximation, and consequently results of calculations using this approximation obey the virial theorem. In the case of Slater exchange, an approximation is made in the application of the variational principle, and as a result the thermodynamic states obtained are not the true equilibrium states for the modified Hartree-Fock system, so that calculations based on the Slater approximation do not obey the virial theorem.

II. CALCULATION OF ENERGY AND PRESSURE

Consider a system of a very large volume V, containing N electrons. The total energy of this system for the modified form of the Hartree-Fock equations may be written as

$$E=\int_0^V -\sum_i \psi_i(\mathbf{r}_i)\,\tfrac{1}{2}\nabla^2\psi_i(\mathbf{r}_1)d\mathbf{r}_1+\tfrac{1}{2}\sum_i\sum_j\int_0^V \frac{\psi_i^*(\mathbf{r}_1)\psi_i(\mathbf{r}_1)\psi_j(\mathbf{r}_2)\psi(\mathbf{r}_2)d\mathbf{r}_1d\mathbf{r}_2}{|\mathbf{r}_1-\mathbf{r}_2|}-\frac{1}{2}\frac{3}{\pi}\left(\frac{3\pi^2}{4}\right)^{1/3}\int_0^V\Big[\sum_{i(\uparrow)}\psi_i^*(\mathbf{r}_1)\psi_i(\mathbf{r}_1)\Big]^{4/3}d\mathbf{r}_1$$
$$-\frac{1}{2}\frac{3}{\pi}\left(\frac{3\pi^2}{4}\right)^{1/3}\int_0^V\Big[\sum_{i(\downarrow)}\psi_i^*(\mathbf{r}_1)\psi_i(\mathbf{r}_1)\Big]^{4/3}d\mathbf{r}_1-\sum_i\sum_\alpha Z_\alpha\int_0^V\frac{\psi_1^*(\mathbf{r}_1)\psi_i(\mathbf{r}_1)d\mathbf{r}_1}{|\mathbf{r}_\alpha-\mathbf{r}_1|}+\tfrac{1}{2}\sum_\alpha\sum_\beta\frac{Z_\alpha Z_\beta}{|\mathbf{r}_\alpha-\mathbf{r}_\beta|}. \quad (1)$$

* Work performed under the auspices of the U. S. Atomic Energy Commission.
[1] W. Kohn and L. J. Sham, Phys. Rev. **140**, A1133 (1965); R. Gaspar, Acta Phys. Acad. Sci. Hung. **3**, 263 (1954).
[2] J. C. Slater, Phys. Rev. **81**, 385 (1951).